IEEE Access
Multidisciplinary ⋮ Rapid Review ⋮ Open Access Journal

Received 21 July 2022, accepted 22 August 2022, date of publication 29 August 2022, date of current version 8 September 2022.

Digital Object Identifier 10.1109/ACCESS.2022.3202530

RESEARCH ARTICLE

Ultra-Wideband and Lightweight Electromagnetic Polarization Converter Based on Multiresonant Metasurface

THI MINH NGUYEN[1,2], THI KIM THU NGUYEN[1,2], DUY TUNG PHAN[3], DAC TUYEN LE[4], DINH LAM VU[1], THI QUYNH HOA NGUYEN[2,5], AND JUNG-MU KIM[5]

[1]Vietnam Academy of Science and Technology, Graduate University of Science and Technology, Cau Giay, Hanoi 10000, Vietnam
[2]School of Engineering and Technology, Vinh University, Vinh, Nghe An 43000, Vietnam
[3]Centre for Wireless Communications, University of Oulu, 90570 Oulu, Finland
[4]Department of Physics, Hanoi University of Mining and Geology, Hanoi 10000, Vietnam
[5]Department of Electronic Engineering, Jeonbuk National University, Jeonju 54896, Republic of Korea

Corresponding authors: Thi Quynh Hoa Nguyen (ntqhoa@vinhuni.edu.vn) and Jung-Mu Kim (jungmukim@jbnu.ac.kr)

This research is supported by Ministry of Education and Training, Vietnam (Grant No. B2022-TDV-04). Thi Kim Thu Nguyen was funded by Vingroup JSC and supported by the PhD scholarship programme of Vingroup Innovation Foundation (VINIF), Institute of Big Data, code VINIF.2021.TS.059. The authors are grateful to supports from the National Research Foundation of Korea (NRF) grant by the Korea government (MSIT) (No. 2021R1A4A1032234).

ABSTRACT Polarization-control devices have attracted considerable interest, however, most of the polarization converters operating at lower frequencies have a heavy design and narrow bandwidth which limits their practical applications. Here we report a simple design of an ultra-wideband and lightweight polarization converter for applications in the S- and C-bands. The proposed converter is designed based on a metasurface structure with the dielectric layer modified to hollow structure to obtain a lightweight design even working at such low frequency. Theoretical analysis and simulation results indicate that the converter can convert the orthogonal polarization transformation of reflected wave. Furthermore, the measurement results show good agreement with the simulation results. The proposed polarization converter can achieve a polarization conversion ratio above 90% in an ultra-wide frequency range from 2 to 8.45 GHz due to multi-resonance modes. These performances are going beyond state of the art in terms of bandwidth and lightweight design, thus it can be applied in various applications in the operating bands.

INDEX TERMS Linear polarization converter, lightweight design, ulta-wideband converter, multi-resonant metasurface, S- and C-bands.

I. INTRODUCTION

Together with frequency, phase, and energy, polarization is one of the crucial characteristics of electromagnetic (EM) waves since it is taken into consideration in most EM applications. Therefore, the controlling polarization state of an EM wave plays an important role to broaden its practical applications. The term EM polarization refers to the oscillating direction of the electric field in a plane perpendicular to the propagated direction of the EM wave. Normally, a polarization converter is used to control the EM polarization. Conventional polarization converters are achieved by using either birefringent crystals based on Faraday effects [1], optical gratings [2], or employing the Brewster [3], [4]. Therefore, the conventional designs are usually heavy-weight, difficult in miniaturization, and narrow bandwidth, which limits their practical applications [5], [6]. Since then, many efforts have been made to overcome the disadvantage of the conventional polarization converters [7], [8], [9], [10], [11], [12], [13], [14], [15], [16], [17], [18]. Among the proposed methods, using metamaterials (MMs) is considered as a potential approach to developing a new class of miniaturized and wideband polarization converter [15], [16], [17], [18].

Metasurface has proved as an effective method to realize lightweight absorber [19], vortex beam generator [20], holograms [21], lens [22], cloaks [23], and surface plasmon

The associate editor coordinating the review of this manuscript and approving it for publication was Zhongyi Guo.

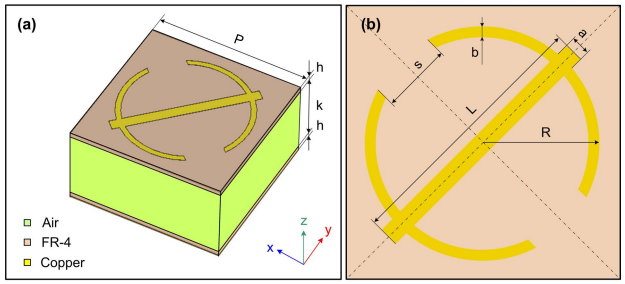

FIGURE 1. Schematic drawings of the designed unit cell of the polarization converter with geometric: (a) 3D-view and (b) top view.

TABLE 1. Optimum parametric value of the unit cell of the polarization converter.

Parameter	P	k	h	a	b	s	L	R
Value (mm)	22.2	10	0.8	1.54	0.75	2.7	10.3	9.3

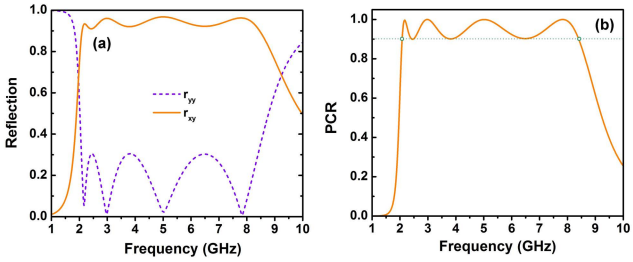

FIGURE 2. (a) Simulated magnitude of co- and cross-polarization reflections and (b) Simulated PCR versus frequency under normal incidence and TE mode.

polariton couplers [24] due to its advantages such as ultrathin thickness and scalable property. Normally, a metasurface is formed by arranging unit cells into a two-dimensional pattern at a surface or interface, therefore, they are considered as a two-dimensional equivalent of metamaterials. Among the different types of metasurface, anisotropic or chiral metasurface has demonstrated a convenient method to control the polarization state of electromagnetic waves. However, the polarization converters based on the anisotropic and chiral metasurfaces shown either a narrow bandwidth or low conversion efficiency [15]. Therefore, most of previous studies on this kind of polarization converter focus on expand the bandwidth by using stacking multilayer structures [16], [17] or using multiple plasmon resonances [13], [25]. However, the multilayer structures also lead to a bulky volume while the polarization based on multile resonances mothod shows a low polarization conversion ratio (PCR) below 50% [13]. Since then, the design of a polarization converter with miniaturized design while maintaining high conversion rate in a wide bandwidth is still a major challenge.

In this work, we present a high conversion efficiency and ultra-wideband polarization converter with a simple and lightweight design. The proposed polarization converter is the linear type that rotates a linearly polarized EM wave into its orthogonal counterpart. The unit cell of the proposed converter is composed of a metallic pattern as a resonator mounted on a hollow FR-4 dielectric substrate to achieve the lightweight characteristic. The multiple resonances that are produced by both electric and magnetic resonances can be used to obtain the ultra-wideband characteristic. The proposed converter shows the PCR above 90% with a relative bandwidth (RBW) of 123.4% in the wide band from 2.0 GHz to 8.45 GHz.

II. DESIGN AND SIMULATION

Figure 1 shows a schematic of the designed unit cell of the proposed polarization converter. The polarization converter's structure consists of a periodic array of an anisotropic metasurface unit cell (not shown here). As shown in Fig. 1(a), the unit cell of the proposed polarization converter is composed of two identical FR-4 substrate layers separated by an air gap. A metallic pattern is etched on the top side of the upper substrate plays as a resonator. Meanwhile, the bottom side of the lower substrate is backed by a continuous metal sheet which plays as a ground plane. The loss tangent and relative dielectric constant of the FR-4 substrate are 0.025 and 4.3, respectively. The metallic pattern plays as a resonator which is composed of two opposite arcs connected by a strip at the center (Fig. 1(b)). The top and bottom layers of unit cell are made of copper, which has a thickness of 0.035 mm and an electric conductivity of 5.96×10^7 S/m. The geometrical parameters of the unit cell are shown in Table 1. It is worth to mention that a thicker dielectric contributes to a lower radiative Q-factor and can therefore enhance the operational bandwidth [26]. However, a unit cell with actual (solid) and thick substrate normally is heavy, therefore, the airgap is introduced here as a solution to achieve the wideband and lightweight characteristics at the same time.

To evaluate the performance of the proposed polarization converter, the commercial CST Microwave Studio 2015 software is performed using a frequency-domain solver. The unit cell boundary conditions are assigned to the x-and y-directions, while open conditions are applied to the z-direction.

In general, the working principle of a linear polarization converter is that it converts most of the incident wave into the reflected wave with a rotating 90° in polarization (cross-polarization). However, there is an amount of reflected wave that does not change the polarization after the reflection (co-polarization); therefore, cross-reflection (r_{xy}) and co-reflection (r_{yy}) coefficients are used to represent the co- and cross-polarization reflected components. Assuming that incident EM wave is y-polarized wave with electric field E_{iy}, then the co- and cross-reflection coefficients are defined as $r_{xy} = |E_{rx}|/|E_{iy}|$, and $r_{yy} = |E_{ry}|/|E_{iy}|$, where $|E_{rx}|$ and $|E_{ry}|$ are the magnitude of the electric field of the reflected wave components along x- and y-axes, respectively.

Fig. 2(a) shows the simulated amplitude of co- and cross-polarization coefficients of the proposed polarization

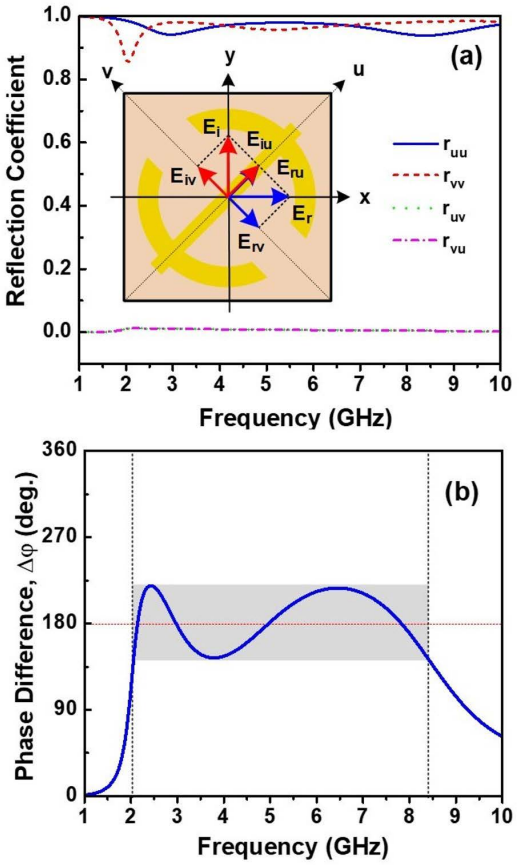

FIGURE 3. (a) Simulated magnitude of the reflection coefficient of *u*- and *v*-components for the proposed polarization converter under normal incidence and TE mode (inset illustrates the working principle of the polarization converter) and (b) Phase difference between r_{uu} and r_{vv}.

converter versus frequency from 1 to 10 GHz under transverse electric (TE) mode. We can observe that the r_{xy} is much bigger than r_{yy} in a band from 2 to 8.45 GHz, which confirms most of the incident wave has been converted to its cross-polarized wave after reflection in this band. In order to evaluate the polarization conversion performance of the proposed polarization converter, we use a PCR which is defined from the co- and cross-reflection coefficients as Eq. 1 [14].

$$PCR = \frac{|r_{xy}|^2}{|r_{xy}|^2 + |r_{yy}|^2} \tag{1}$$

Fig. 2(b) illustrates the simulated PCR of the polarization converter. The simulation is carried out in the band from 2 to 10 GHz with the incident wave coming from the normal direction and under TE mode. We can observe a nearly perfect PCR above 90% is achieved from 2 to 8.45 GHz which fully covers both the S- and C- bands.

To understand the working principle of the proposed polarization converter, the simulated amplitude and phase difference of the reflection coefficients are given out as Fig. 3. Assuming that the incident wave is polarized along the y-axis and propagates perpendicular to the top layer of the polarization converter along the z-direction. As shown in 3(a), the incident electric field (E_i) and reflected electric field (E_r) of the EM wave can be decomposed into two mutually perpendicular components in the *uv*-coordinate system as Eqs. 2 and 3, respectively.

$$E_i = E_{iu} + E_{iv} \tag{2}$$

$$E_r = E_{ru} + E_{rv} = r_{uu}E_{iu} + r_{vv}E_{iv} \tag{3}$$

where r_{uu} and r_{vv} are the reflected coefficients along the *u*-axis and *v*-axis, which can be defined as $r_{uu} = |E_{ru}|/|E_{iu}|$, and $r_{vv} = |E_{rv}|/|E_{iv}|$.

Since a low loss dielectric ($tan\delta = 0.025$) is used for the polarization converter, the energy loss of the incident EM wave can be neglected; Therefore, the amplitude of r_{uu} and r_{vv} can be assumed to unit ($|r_{uu}| = |r_{vv}| = 1$). Also, due to the proposed polarization converter is an asymmetrical structure, it can be considered as an anisotropic material with dispersive relative permittivity and permeability results in a phase difference ($\Delta\varphi$) between r_{uu} and r_{vv} [27]. Then, we have the relation between r_{uu} and r_{vv} as: $r_{vv} = r_{uu}\, e^{j\Delta\varphi}$. Thus, Eq. 3 can be rewritten as Eq. 4.

$$E_r = r_{u_u}E_{iu} + r_{uu}e^{j\Delta\varphi}E_{iv} \tag{4}$$

When $|\Delta\varphi| = 180° + 2k\pi$ (k is integer), combine Eqs. 3 and 4 we have $E_{ru} = r_{uu}E_{iu}$ and $E_{rv} = -r_{uu}E_{iv}$. It means that either E_{ru} or E_{rv} is opposite to their corresponded incident direction, leading to the synthetic reflected electric field (E_r) is rotated exactly 90° compared to the incidence as depicted in inset of Fig. 3(a).

To verify this theoretical analysis, we simulate the magnitude and phase difference of the reflection of *u*- and *v*-components for the converter under normal incidence. As shown in Fig. 3(a), the co-reflection amplitudes of *u*- and *v*-polarized waves, r_{uu} and r_{vv}, are nearly equal 1 in an ultra-wide bandwidth from 2 to 8.45 GHz as we theoretically predicted. Moreover, the cross-reflection coefficient between *u*- and *v*-polarizations, r_{uv} and r_{vu}, are nearly zero in the band which confirms no cross-polarization exists at *u*- and *v*- polarizations. Fig. 3(b) gives the phase difference $\Delta\varphi$ between r_{uu} and r_{vv} over frequency. As shown in Fig. 3b, we get $180°-40° \leq \Delta\varphi \leq 180°+40°$ from 2 GHz to 8.45 GHz. The phase difference is equal 180° at 2.16 GHz, 2.98 GHz, 5.0 GHz, and 7.83 GHz which the same with four resonant frequencies of the polarization converter.

In additional, to better qualitatively verdict the polarization state of EM wave, ellipticity (η) and polarization azimuth angle (θ) for the y-polarize and normal incidence also are investigated, which are determined as Eqs. 5 and 6 [28], [29].

$$\eta = \frac{1}{2}\arcsin\left(\frac{2 \times p_r \times \sin(\Delta\varphi)}{1 + |p_r|^2}\right) \tag{5}$$

$$\theta = \frac{1}{2}\arctan\left(\frac{2 \times p_r \times \cos(\Delta\varphi)}{1 - |p_r|^2}\right) \tag{6}$$

where $|p_r| = |r_{xy}|/|r_{yy}|$ and $\Delta\varphi$ is the phase difference between r_{xy} and r_{yy}. Theta is the rotation angle of the electric

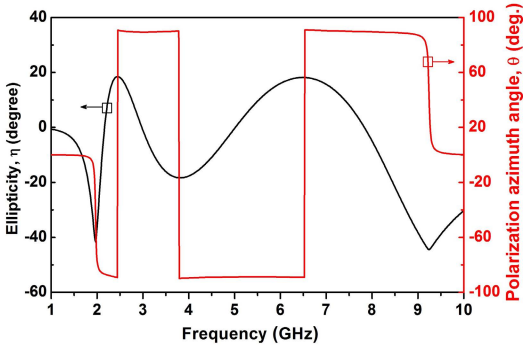

FIGURE 4. Ellipticity η and polarization azimuth angles θ for y-polarization.

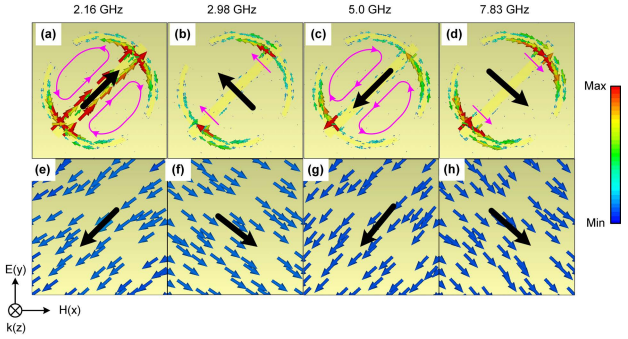

FIGURE 5. Surface current distributions on the (a)-(d) top layers and (e)-(h) metallic ground sheet of the polarization converter unit cell at the four resonant frequencies.

field direction of the reflected wave with respect to the electric field direction of the incident waves, whereas eta denotes the polarization state of the reflecting wave. When $\eta = 0°$, the reflected wave has linear polarization; otherwise, it has another type of polarization. As a result, the y-polarization wave can be transformed into its x-polarization counterpart if $\eta = 0°$ and $\theta = \pm 90°$. The calculated θ and η are illustrated in Fig. 4 which shows that the ellipticity of the incident y-polarized wave stands less than 18° from 2.0 to 8.45 GHz at the whole frequency band while the polarization azimuth angle keeps nearly 90° or −90° in the band.

Moreover, in order to explore the physical mechanism behind the ultra-wideband polarization conversion behavior of the proposed converter, we simulate the surface current distributions on the metallic pattern (top layer) and the ground plane (bottom layer) at the four resonant frequencies (Fig. 5). As shown in Figs. 5(a), (e) and Figs. 5(b), (f), the surface currents on the top layer are anti-parallel to those on the ground plane at 2.16 GHz and 2.98 GHz. The anti-parallel currents together form a loop current in the dielectric layers, which is considered as magnetic resonance [22]. In reversely, the surface currents on the top layer are parallel to those on the ground plane at 5.0 GHz and 7.83 GHz as shown in Figs. 5(c), (g) and Figs. 5(d), (h). The parallel currents on the top and the bottom layers will form an E-field in the substrate layer which indicates the electric resonance occurs [30]. Hence, these two higher resonances are originated by electric resonance. Furthermore, two loops of currents (left loop is anticlockwise and right is clockwise) appear in Fig. 5(a) (pink color), while those in Fig. 5(c) are the same just with the reverse loop of current (left loop is clockwise and right is anticlockwise), which typically exhibits the feature of magnetic resonance. However, the excited magnetic fields are created by these loops is antiparallel and therefore cancel each other. Moreover, the currents in two arm of arcs both flow to the up-left (Fig. 5(b)), while the direction of currents are with the opposite direction (Fig. 5(d)), displaying the characteristic of electric resonance. The synthetic electric field is the same direction with the incident electric field at the resonant frequency of 2.98 GHz. It indicates that the magnetic resonance is mainly contributed to this resonant frequency [31]. However, the synthetic electric field is the opposite of the incident electric field at 7.83 GHz (Fig. 5(d)), indicating that the excited electric field is stronger than the incident electric field. This phenomenon proves that an electric resonance is excited at 7.83 GHz [31]. It is can be concluded that the overlap of the four polarization rotation resonances is responsible for the ultra-wideband polarization conversion of the proposed polarization converter.

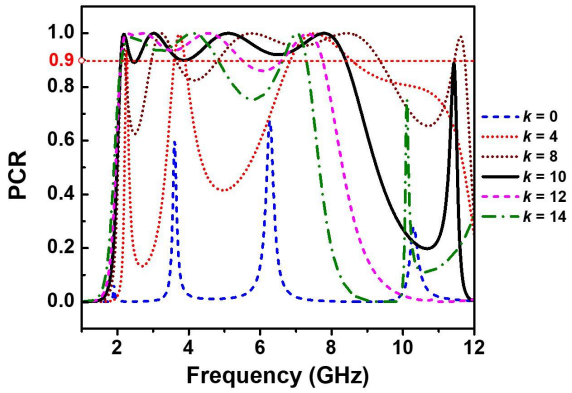

FIGURE 6. PCR of the proposed polarization converter at different airgap thicknesses under TE mode.

To further investigate the contribution of the airgap layer on the conversion performance of the proposed polarization converter, we simulate the PCR of the converter at different values of the airgap thickness. As shown in Fig. 6, the polarization converter without the airgap shows four separated and narrow peaks in the band from 0 to 12 GHz with a low performance. By introducing the airgap, the PCR level of the peaks are improved significantly. Moreover, the lowest resonances are nearly unchanged when the thickness of the airgap varies from 4 to 14 mm. In contrast, the other resonances move to lower frequency band with the increase in the thickness of airgap forming a wide band PCR spectrum. However, with the airgap above 10 mm, the resonances are too close to each other results in the PCR bandwidth of the proposed polarization converter shrank. The effects of

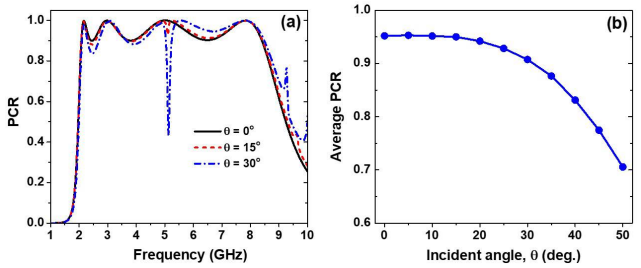

FIGURE 7. (a) Simulated PCR versus frequency of the polarization conversion as a function of the incident angle and (b) Average PCR of the polarization converter in the band versus incident angle under TE mode.

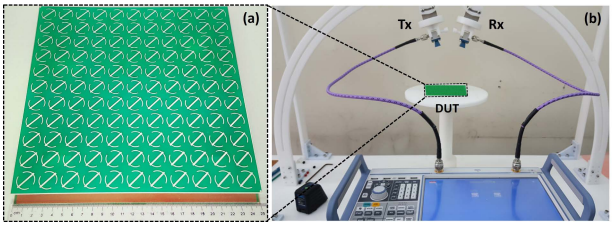

FIGURE 8. (a) Photo of fabricated polarization converter which consists of 11 × 11 unit cells, and (b) Measurement setup for the fabricated prototype.

the air-gap thickness on the performance of the proposed polarization converter can be explained by the transmission line theory. The equivalent circuit of a unit cell of proposed structure can be illustrated in [32]. The admittance of metallic resonant patch and the admittance of the FR4 dielectric slabs and the airgap are connected in parallel to form the input admittance of the proposed structure. When the imaginary part of the input admittance is equal to zero, resonances can be produced [33]. The size and shape of the resonator patch are also optimized and fixed the its admittance. To meet the lightweight requirement, the thickness of FR-4 substrates are fixed to 0.8 mm. As a result, the resonant frequencies can be adjusted using the thickness of the airgap (k) [32]. Furthermore, an optimized airgap thickness can be found to create the resonances that give the largest impedance matching and yield the widest broadband characteristic. As shown in Fig. 6, the optimum airgap thickness for the designed structure is obtained at $k = 10$ mm for the best PCR performance.

It is also important to explore the effect of incident angles on the proposed converter performance. Fig. 7(a) shows the PCR of the proposed polarization converter versus frequency at different values of the incident angle. The simulated PCR is carried out under the condition that the electric field of the incident wave parallels to the y-axis (y-polarized). As shown in Fig. 7(a), the PCR of the polarization converter slightly decreases when the incident angle changes from the normal direction (0°) to 30°. In general, the PCR of the polarization converter is maintained above 85% in the ultra-wideband with the incident angle up to 30°, except a very narrow frequency band at 5 GHz. It can see that there is a distinct dip around 5 GHz appeared in the PCR spectrum, which indicates that the incident wave is strongly absorbed [27], [30]. It was reported that the EM absorption is caused by an extra resonance between the metallic ground and metasurfaces [34].

We also calculate the average simulated PCR on the working band of 2 o 8.45 GHz under different incident angles using Eq.7:

$$PCR(\theta) = \sum_{i=1}^{M} PCR(f_i) \tag{7}$$

where $PCR(f_i)$ and M are the PCR at discrete frequency points f_i and the number of discrete frequency points within the working band, respectively; $PCR(\theta)$ is average simulated PCR under incident angle of θ.

Fig. 7(b) shows the average PCR of the polarization converter under TE polarization in the ultra-wideband from 2 GHz to 8.45 GHz as a function of the incident angle. The achieved average PCR of the polarization is higher than 90% with the incident angle up to 30°, and it is still maintained a higher 85% for a wide incident angle up to 38°. This result confirms that the proposed polarization converter exhibits a stable polarization conversion with respect to variations in the incidence angle.

III. EXPERIMENTAL RESULTS

Fig. 8 illustrates the photo of the fabricated polarization converter and the measurement setup for the fabricated prototype as a device under test (DUT). The proposed converter is fabricated by a standard printed circuit board (PCB) manufacturing process which consists of an 11 × 11 unit-cell that corresponds to the dimensions of 244.2 × 244.2 mm^2. The unit cell parameters of the fabricated sample are the same in Tab. 1. To prevent our fabricated sample from any possible degradation, oxidation, or corrosion, the PCB tinning which is the process of coating copper metasurface with thin layer of tin, is carried out and the result of the sample surface after the tinning process is shown in Fig. 8 (a). The measurement of the DUT is performed using a vector network analyzer (Rohde and Schwarz ZNB20) associated with two standard-gain horn antennas as transmitter (Tx) and receiver (Rx) to determine the reflection coefficients. The DUT is located 0.5 m away from the antennas to satisfy a far-field condition. Due to the measurements are performed in the free space, the measurement system is calibrated with this condition to embed the effect of the environment. The measured PCR of the DUT is determined from the co- and cross-reflection coefficients as described in Eq. 1. The measurements are taken in the frequency range from 1 to 10 GHz. The detailed description of the measurement setup can be found in [35].

Fig. 9 shows the measurement result at a oblique angle of 10°, which is in a good agreement with the simulation. As shown in Figs. 9(a) and (b), measured magnitude of co- and cross-reflection coefficients are above 0.9 and bellow 0.3 in a very wide frequency range from 2 to 8.45 GHz. This result correspond to measured PCR results under transverse electric (TE) and transverse magnetic (TM) modes are higher

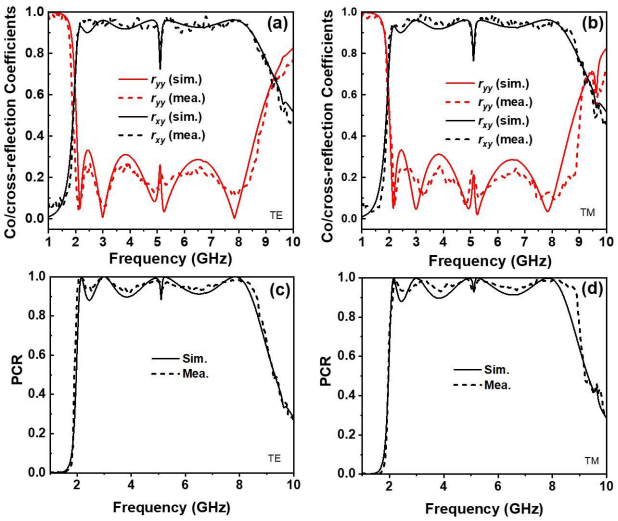

FIGURE 9. Measured reflection coefficients and PCR of the fabricated polarization converter under (a), (c) TE mode and (b), (d) TM mode.

TABLE 2. Performance of proposed polarization converter and existing works in literature.

Ref.	BW (GHz)	RBW (%)	Thickness (solid parts)	Size of unit-cell	Weight factor
[27]	7−19.5	94.3	$0.15\lambda_c$	$0.40\lambda_c$	5.2
[37]	8.44−24.96	98.9	$0.17\lambda_c$	$0.36\lambda_c$	4.8
[38]	14.3−43.2	100.5	$0.15\lambda_c$	$0.60\lambda_c$	11.7
[39]	6.67−17.1	87.8	$0.14\lambda_c$	$0.48\lambda_c$	7.0
[40]	8.85−18.85	72.2	$0.12\lambda_c$	$0.32\lambda_c$	2.7
[41]	490−1880	117.3	$0.18\lambda_c$	$0.4\lambda_c$	6.3
[42]	5.7−10.3	57.5	$0.08\lambda_c$	$0.18\lambda_c$	1.3
This work	**2−8.45**	**123.4**	$\mathbf{0.03}\lambda_c$	$\mathbf{0.39}\lambda_c$	**1.0**

than 0.9 in the band. The measurement demonstrates that the proposed polarization converter is a highly efficient linear polarization conversion.

Table 2 gives a performance comparison to confirm the advantages of the proposed design compared to existing broadband polarization converters which were recently reported in the literature. The comparison is carried out in terms of operating bandwidth with an efficiency above 90%, relative bandwidth, conversion efficiency, total thickness of solid parts, and size of unit cell. The operating bandwidth (BW) and relative bandwidth (RBW) are defined as $RBW = (f_u - f_l)/f_c$, respectively where f_u and f_l are upper and lower frequencies correspond to a conversion efficiency above 90% and $f_c = (f_u + f_l)/2$ is center frequency of the operating band. Moreover, in order to judge the light-weight characteristic of converter designs, we give the weight factor (w) which is proportional to thickness excluding air-gap (t_{solid}) and periodicity of the unit cell (P) as $w \propto t_{solid}P^2$. For the t_{solid}, we only consider thickness of the substrate since the metal layer is very thin compare to the subtrate layer. The weight factor of this work is defined as standard (1.0); therefore, the value of the factor below or above 1 indicates a how much the design is lighter- or heavier-weight compare to the proposed polarization converter, respectively. As indicated in Table 2, the proposed polarization converter operates at lowest frequency band with highest fractional bandwidth and has the most lightweight design among them.

IV. CONCLUSION

We present an ultra-wideband and high efficiency polarization converter for S- and C- bands applications. By introducing a hollow dielectric layer to a simple metasurface resonator, the polarization converter shows a very lightweight design even working at a relatively low frequency. Firstly, theoretical analysis and simulation are carried out to explain the working mechanism of the polarization converter. Then, the polarization converter is fabricated and the experimental results are carried out with good agreement with the simulation results. The results show that the proposed polarization converter converts linear-polarized incident EM waves into its cross-polarized reflective counterparts with high polarization conversion with a polarization conversion ratio above 90% in an ultrawide frequency range from 2 to 8.45 GHz. This operating frequency band corresponds to a relative bandwidth of 123.4% and entirely covers both the S- and C-bands. Compared with the available broadband designs, the proposed polarization converter shows excellent performance in terms of simple and lightweight design and ultrawide bandwidth. The advantages demonstrate great potential for applications in microwave communications, imaging systems, and remote sensors.

REFERENCES

[1] P. Yeh, "Electromagnetic propagation in birefringent layered media," *J. Opt. Soc. Amer.*, vol. 69, no. 5, pp. 742–756, 1979.
[2] T. Meissner and F. J. Wentz, "Polarization rotation and the third Stokes parameter: The effects of spacecraft attitude and Faraday rotation," *IEEE Trans. Geosci. Remote Sens.*, vol. 44, no. 3, pp. 506–515, Mar. 2006.
[3] M. R. Andrews, P. P. Mitra, and R. de Carvalho, "Tripling the capacity of wireless communications using electromagnetic polarization," *Nature*, vol. 409, pp. 316–318, Jan. 2001.
[4] A.-C. Ji, X. C. Xie, and W. M. Liu, "Quantum magnetic dynamics of polarized light in arrays of microcavities," *Phys. Rev. Lett.*, vol. 99, no. 18, Nov. 2007, Art. no. 183602.
[5] J. Xu, T. Li, F. Lu, S. Wang, and S. Zhu, "Manipulating optical polarization by stereo plasmonic structure," *Opt. Exp.*, vol. 19, no. 2, pp. 748–756, 2011.
[6] M. Mutlu and E. Ozbay, "A transparent 90° polarization rotator by combining chirality and electromagnetic wave tunneling," *Appl. Phys. Lett.*, vol. 100, no. 5, Jan. 2012, Art. no. 051909.
[7] B. Lin, L. Lv, J. Guo, Z. Liu, X. Ji, and J. Wu, "An ultra-wideband reflective Linear-to-circular polarization converter based on anisotropic metasurface," *IEEE Access*, vol. 8, pp. 82732–82740, 2020.
[8] W. Mo, X. Wei, K. Wang, Y. Li, and J. Liu, "Ultrathin flexible terahertz polarization converter based on metasurfaces," *Opt. Exp.*, vol. 24, no. 12, pp. 13621–13627, Jun. 2016.
[9] L. Dai, Y. Zhang, H. Zhang, and J. F. O'Hara, "Broadband tunable terahertz cross-polarization converter based on dirac semimetals," *Appl. Phys. Exp.*, vol. 12, no. 7, Jul. 2019, Art. no. 075003.
[10] A. K. Fahad, C. Ruan, R. Nazir, M. Saleem, T. U. Haq, S. Ullah, and W. He, "Ultra-thin metasheet for dual-wide-band linear to circular polarization conversion with wide-angle performance," *IEEE Access*, vol. 8, pp. 163244–163254, 2020.
[11] X. Huang, H. Yang, D. Zhang, and Y. Luo, "Ultrathin dual-band metasurface polarization converter," *IEEE Trans. Antennas Propag.*, vol. 67, no. 7, pp. 4636–4641, Jul. 2019.
[12] P. Xu, S.-Y. Wang, and G. Wen, "A linear polarization converter with near unity efficiency in microwave regime," *J. Appl. Phys.*, vol. 121, no. 14, Apr. 2017, Art. no. 144502.

[13] H. Chen, J. Wang, H. Ma, S. Qu, Z. Xu, A. Zhang, M. Yan, and Y. Li, "Ultra-wideband polarization conversion metasurfaces based on multiple plasmon resonances," *J. Appl. Phys.*, vol. 115, Apr. 2014, Art. no. 154504.
[14] T. Q. H. Nguyen, T. K. T. Nguyen, T. Q. M. Nguyen, T. N. Cao, H. L. Phan, N. M. Luong, D. T. Le, X. K. Bui, C. L. Truong, and D. L. Vu, "Simple design of a wideband and wide-angle reflective linear polarization converter based on crescent-shaped metamaterial for Ku-band applications," *Opt. Commun.*, vol. 486, May 2021, Art. no. 126773.
[15] Z. Zhang, J. Wang, X. Fu, Y. Jia, H. Chen, M. Feng, R. Zhu, and S. Qu, "Single-layer metasurface for ultra-wideband polarization conversion: Bandwidth extension via Fano resonance," *Sci. Rep.*, vol. 11, no. 1, pp. 1–8, Dec. 2021.
[16] F. Zhang, G.-M. Yang, and Y.-Q. Jin, "Microwave polarization converter with multilayer metasurface," in *Proc. 14th Eur. Conf. Antennas Propag. (EuCAP)*, Mar. 2020, pp. 1–4.
[17] L. S. Ren, Y. C. Jiao, F. Li, J. J. Zhao, and G. Zhao, "A dual-layer T-shaped element for broadband circularly polarized reflectarray with linearly polarized feed," *IEEE Antennas Wireless Propag. Lett.*, vol. 10, pp. 407–410, 2011.
[18] C. Fu, Z. Sun, L. Han, C. Liu, T. Sun, and P. K. Chu, "High-efficiency dual-frequency reflective linear polarization converter based on metasurface for microwave bands," *Appl. Sci.*, vol. 9, no. 9, p. 1910, May 2019.
[19] Z. Li, B. Li, Q. Zhao, and J. Zhou, "A metasurface absorber based on the slow-wave effect," *AIP Adv.*, vol. 10, no. 4, Apr. 2020, Art. no. 045311.
[20] K. Cheng, Z.-D. Hu, X. Kong, X. Shen, and J. Wang, "High performance reflective microwave split-square-ring metasurface vortex beam generator," *Opt. Commun.*, vol. 507, Mar. 2022, Art. no. 127631.
[21] J. Burch, J. Ma, R. I. Hunter, S. A. Schulz, D. A. Robertson, G. M. Smith, J. Wang, and A. Di Falco, "Flexible patches for mm-wave holography," *Appl. Phys. Lett.*, vol. 115, no. 2, Jul. 2019, Art. no. 021104.
[22] D. Neshev and I. Aharonovich, "Optical metasurfaces: New generation building blocks for multi-functional optics," *Light, Sci. Appl.*, vol. 7, no. 1, pp. 1–5, Dec. 2018.
[23] H. Chu, Q. Li, B. Liu, J. Luo, S. Sun, Z. H. Hang, L. Zhou, and Y. Lai, "A hybrid invisibility cloak based on integration of transparent metasurfaces and zero-index materials," *Light, Sci. Appl.*, vol. 7, no. 1, pp. 1–8, Dec. 2018.
[24] H. Chen, H. Ma, J. Wang, Y. Li, M. Feng, Y. Pang, M. Yan, and S. Qu, "Broadband spoof surface plasmon polariton couplers based on transmissive phase gradient metasurface," *J. Phys. D, Appl. Phys.*, vol. 50, no. 37, Sep. 2017, Art. no. 375104.
[25] M. Feng, J. Wang, H. Ma, W. Mo, H. Ye, and S. Qu, "Broadband polarization rotator based on multi-order plasmon resonances and high impedance surfaces," *J. Appl. Phys.*, vol. 114, Aug. 2013, Art. no. 074508.
[26] S. A. Tretyakov, "Metasurfaces for general transformations of electromagnetic fields," *Philos. Trans. Roy. Soc. London A, Math. Phys. Sci.*, vol. 373, no. 2049, 2015, Art. no. 20140362.
[27] J. Xu, R. Li, J. Qin, S. Wang, and T. Han, "Ultra-broadband wide-angle linear polarization converter based on H-shaped metasurface," *Opt. Exp.*, vol. 26, no. 16, pp. 20913–20919, 2018.
[28] Z. Xiao, H. Zou, X. Zheng, X. Ling, and L. Wang, "A tunable reflective polarization converter based on hybrid metamaterial," *Opt. Quantum Electron.*, vol. 49, no. 12, p. 401, Dec. 2017.
[29] H. Shi, J. Li, A. Zhang, J. Wang, and Z. Xu, "Broadband cross polarization converter using plasmon hybridizations in a ring/disk cavity," *Opt. Exp.*, vol. 22, no. 17, pp. 20973–20981, 2014.
[30] X. Gao, X. Han, W.-P. Cao, H. O. Li, H. F. Ma, and T. J. Cui, "Ultrawideband and high-efficiency linear polarization converter based on double V-shaped metasurface," *IEEE Trans. Antennas Propag.*, vol. 63, no. 8, pp. 3522–3530, Aug. 2015.
[31] Q. Chen, S. Bie, W. Yuan, Y. Xu, H. Xu, and J. Jiang, "Low frequency absorption properties of a thin metamaterial absorber with cross-array on the surface of a magnetic substrate," *J. Phys. D, Appl. Phys.*, vol. 49, no. 42, Oct. 2016, Art. no. 425102.
[32] D. T. Phan, T. K. T. Nguyen, N. H. Nguyen, D. T. Le, X. K. Bui, D. L. Vu, C. L. Truong, and T. Q. H. Nguyen, "Lightweight, ultra-wideband, and polarization-insensitive metamaterial absorber using a multilayer dielectric structure for C- and X-band applications," *Phys. Status Solidi B*, vol. 258, no. 10, 2021, Art. no. 425102.
[33] Z. Yao, S. Xiao, Z. Jiang, L. Yan, and B.-Z. Wang, "On the design of ultrawideband circuit analog absorber based on quasi-single-layer FSS," *IEEE Antennas Wireless Propag. Lett.*, vol. 19, no. 4, pp. 591–595, Apr. 2020.
[34] M. Diem, T. Koschny, and C. M. Soukoulis, "Wide-angle perfect absorber/thermal emitter in the terahertz regime," *Phys. Rev. B, Condens. Matter*, vol. 79, no. 3, Jan. 2009, Art. no. 033101, doi: 10.1103/PhysRevB.79.033101.
[35] T. K. T. Nguyen, T. M. Nguyen, H. Q. Nguyen, T. N. Cao, D. T. Le, X. K. Bui, S. T. Bui, C. L. Truong, D. L. Vu, and T. Q. H. Nguyen, "Simple design of efficient broadband multifunctional polarization converter for X-band applications," *Sci. Rep.*, vol. 11, no. 1, pp. 1–12, Dec. 2021.
[36] Y. Zhao, B. Qi, T. Niu, Z. Mei, L. Qiao, and Y. Zhao, "Ultra-wideband and wide-angle polarization rotator based on double W-shaped metasurface," *AIP Adv.*, vol. 9, no. 8, Aug. 2019, Art. no. 085013.
[37] H. Dai, Y. Zhao, H. Sun, J. Chen, Y. Ge, and Z. Li, "An ultra-wideband linear polarization conversion metasurface," *Jpn. J. Appl. Phys.*, vol. 57, no. 9, Sep. 2018, Art. no. 090311.
[38] J. Xu, R. Li, S. Wang, and T. Han, "Ultra-broadband linear polarization converter based on anisotropic metasurface," *Opt. Exp.*, vol. 26, no. 20, pp. 26235–26241, Oct. 2018.
[39] F. Long, S. Yu, N. Kou, C. Zhang, Z. Ding, and Z. Zhang, "Efficient broadband linear polarization conversion metasurface based on %-shape," *Microw. Opt. Technol. Lett.*, vol. 62, no. 1, pp. 226–232, Jan. 2020.
[40] Z. Xu, H. Sheng, Q. Wang, L. Zhou, and Y. Shen, "Terahertz broadband polarization converter based on the double-split ring resonator metasurface," *Social Netw. Appl. Sci.*, vol. 3, no. 9, pp. 1–7, Sep. 2021.
[41] J. Zhao and Y. Cheng, "A high-efficiency and broadband reflective 90° linear polarization rotator based on anisotropic metamaterial," *Appl. Phys. B, Lasers Opt.*, vol. 122, no. 10, pp. 1–7, Oct. 2016.

THI MINH NGUYEN received the B.S. degree from the University of Engineering and Technology, Vietnam National University, in 2003, and the M.Sc. degree from Le Quy Don University, Hanoi, Vietnam, in 2011. She is currently pursuing the Ph.D. degree with the Vietnam Academy of Science and Technology, Graduate University of Science and Technology, Hanoi. Her research interests include multi-functional metasurfaces for absorber and polarization converter.

THI KIM THU NGUYEN received the B.S. degree from Vinh University, Vinh, Vietnam, in 2003, and the M.Sc. degree from Le Quy Don University, Hanoi, Vietnam, in 2011. She is currently pursuing the Ph.D. degree with the Vietnam Academy of Science and Technology, Graduate University of Science and Technology, Hanoi. Her research interests include metasurface absorber and polarization converter.

DUY TUNG PHAN received the Ph.D. degree from the Seoul National University of Science and Technology (SeoulTech), South Korea, in 2021. He is currently working as a Postdoctoral Fellow with the Centre for Wireless Communications, University of Oulu, Finland. His main research interests include EMI/EMC, metasurface-based polarization converters and absorbers, and reconfigurable intelligent surfaces for mmWave and sub-THz applications.

DAC TUYEN LE received the Ph.D. degree from National Chung Cheng University, Taiwan, in 2012. He is currently an Associate Professor of physics with the Hanoi University of Mining and Geology. His research interests include metamaterials and photonic crystals.

DINH LAM VU received the Ph.D. degree in materials science from the Institute of Materials Sciences, Vietnam Academy of Science and Technology (VAST), Vietnam, in 2006. He was a Postdoctoral Fellow with Hanyang University, South Korea. He is currently a Full Professor with VAST. He has published over 200 peer-reviewed papers. His research interests include metamaterials and their applications.

THI QUYNH HOA NGUYEN received the Ph.D. degree in materials engineering from Chungnam National University, South Korea, in 2009. She is currently an Associate Professor with Vinh University. Her research interests include synthesis and application of advanced functional materials into electronic, energy, and RF/microwave devices.

JUNG-MU KIM was born in Jeonju, South Korea, in 1977. He received the B.S. degree in electronic engineering from Ajou University, Suwon, South Korea, in 2000, and the M.S. and Ph.D. degrees in electrical engineering and computer science from Seoul National University, Seoul, South Korea, in 2002 and 2007, respectively. From 2007 to 2008, he was a Postdoctoral Fellow with The University of California at San Diego. In 2008, he joined as a faculty with the Division of Electronic Engineering, Jeonbuk National University, Jeonju, where he is currently a Full Professor. His research interests include IMU, SPR sensor, RF MEMS for 5G and ink-jet printing, and 3D printing-based printed electronics.